Pré-Publicações do Departamento de Matemática
Universidade de Coimbra
Preprint Number 04–17

EFFECT OF BOUNDARY VORTICITY DISCRETISATION ON EXPLICIT STREAM-FUNCTION VORTICITY CALCULATIONS

ERCÍLIA SOUSA AND IAN SOBEY

Abstract: The numerical solution of the time dependent Navier–Stokes equations in terms of the vorticity and a stream function is a well tested process to describe two-dimensional incompressible flows, both for fluid mixing applications and for studies in theoretical fluid mechanics. In this paper we consider the interaction between the unsteady advection-diffusion equation for the vorticity, the Poisson equation linking vorticity and stream-function and the approximation of the boundary vorticity, examining from a practical viewpoint, global error and global iteration stability. Our results show that error is dominated by the largest error in any of the three parts of the process and that most schemes have very similar global stability constraints although there may be small stability gains from the choice of method to determine boundary vorticity.

Keywords: Navier-Stokes; vorticity boundary conditions, finite differences; stability.

1. Introduction

While the majority of current fluid flow calculations are oriented towards three dimensional flow fields, there remain an important group of simulations of two dimensional unsteady laminar flows: either for applications which are approximately two dimensional or for the intrinsic relevance of two-dimensional flow to theoretical fluid mechanics, see for instance Ottino [1]. In calculating two dimensional flow there are significant advantages in using a stream-function vorticity formulation of the Navier–Stokes equations rather than a velocity-pressure formulation: the continuity equation is automatically satisfied, only one advection equation has to be solved and there is no difficulty in matching a pressure to the velocity field. In regular geometries (or irregular geometries using a conformal map) the use of a finite difference scheme to integrate the stream-function vorticity equations is straight forward except for one important area: the treatment of the boundary vorticity.

Received May 19, 2004.
ES was partially supported by Centro de Matemática da Universidade de Coimbra

The purpose of this paper is to extend studies of the effect of different discretisation of the vorticity boundary conditions for the unsteady incompressible Navier-Stokes equations in the stream-function vorticity formulation. We are especially interested in understanding the global stability properties of explicit time marching schemes using various methods for dealing with the spatially implicit vorticity boundary condition, although in principle, our methods could be applied to implicit time marching schemes. With this purpose we build a matrix form for the system of equations which couples together the advection-diffusion equation for the vorticity, the Poisson equation for the stream-function and the vorticity boundary condition to provide a global iteration matrix; we then study the properties of that matrix for two particular flows. While stability is the primary focus of this work we also note in passing some results on accuracy which are in accordance with existing results although with some new data.

There are many studies of the stream-function vorticity formulation for the Navier-Stokes equations and a substantial literature on the subject, from the seminal work of Thom [2] through to texts on computational fluid mechanics, ranging from the early text Roache [3] to the more recent Peyret and Taylor [4]. The basic method is also reviewed in papers such as Orszag and Israeli [5] and Gresho [6].

The way vorticity is handled at a boundary is extremely important from a physical point of view as it reflects the mechanism of vorticity generation at a boundary. The difficulty with a vorticity formulation is the lack of natural boundary condition on the vorticity since a no-slip boundary condition does not have a simple counterpart in terms of the vorticity. In order to complete the discrete formulation is nevertheless necessary to impose a numerical boundary condition on the vorticity. Perhaps the most well known numerical vorticity boundary condition is that given by Thom [2] which comes from a quadratic polynomial approximation of the stream-function near a boundary. The approximation is constrained to satisfy the correct normal derivative and then applied at the first interior point from the boundary. This type of numerical boundary condition has been analysed by Hou and Wetton [7], associated with a central scheme for the vorticity equation, and shown to yield second order accurate solutions. Later Wang and Liu [8] studied the Wilkes-Pearson formula associated with the central differences and a fourth order scheme with Briley's formula. Other work that has focused on the role of vorticity boundary conditions is in for example: Weinan and Liu

[9] or Napolitano et al. [10]. More recently Li and Wang [11] have generalised vorticity boundary conditions to curved boundary domains. There is also significant work on steady solutions and particularly their accuracy in Spotz [12].

The plan of this paper is to briefly recap the formulation of the global iteration matrix for the Navier Stokes equations (the idea was first explored in Sousa and Sobey [13] for a one-dimensional analogue of the stream-function vorticity equations), to consider a number of well known discretisations (of both the vorticity transport equation and the boundary vorticity) and then to consider two cavity type flows, one an exact solution of the Navier–Stokes equations and one a cavity flow driven by one wall moving uniformly, examining variation of the solution with numerical parameters and stability of explicit finite difference schemes for these flows.

2. Global iteration matrix formulation

In this section we derive a global iteration matrix for the discretised form of the advection-diffusion equation, the Poisson equation between the stream-function and the vorticity and the boundary vorticity method, also considering briefly some conditions for stability of the global iteration.

2.1. Flow equations. We consider incompressible viscous flow in a two-dimensional domain without inflow or outflow. The motion of the fluid is governed by the Navier-Stokes equations,

$$\begin{aligned} \frac{\partial \mathbf{u}}{\partial t} + (\mathbf{u}\cdot\nabla)\mathbf{u} &= -\nabla p + \frac{1}{Re}\nabla^2\mathbf{u}, \\ \nabla\cdot\mathbf{u} &= 0, \end{aligned} \tag{1}$$

where $\mathbf{u} = \mathbf{u}(x,y,t) = (u(x,y,t), v(x,y,t))$ is a non-dimensional velocity field, $p = p(x,y,t)$ is a non-dimensional pressure, and Re is a Reynolds number. In a bounded domain Ω enclosed by a boundary $\partial\Omega$, the impermeability of the boundaries and the no-slip condition implies that

$$\mathbf{u}(x,y,t) = \mathbf{u}_W(x,y,t), \quad \text{for} \quad (x,y) \in \partial\Omega, \quad t > 0, \tag{2}$$

where $\mathbf{u}_W$ denotes the boundary velocity.

In terms of the vorticity field $\omega = v_x - u_y$, the momentum equations provide a vorticity equation,

$$\frac{\partial \omega}{\partial t} + u\frac{\partial \omega}{\partial x} + v\frac{\partial \omega}{\partial y} = \frac{1}{Re}\nabla^2\omega. \tag{3}$$

The fluid velocity, $\mathbf{u} = (u, v)$ is obtained from

$$u = \frac{\partial \psi}{\partial y}, \quad v = -\frac{\partial \psi}{\partial x}, \tag{4}$$

where $\psi(x, y, t)$ is a stream-function, which is connected to the vorticity ω, by a Poisson equation

$$\omega = -\nabla^2 \psi, \tag{5}$$

where without inflow or outflow in the cavity flows we consider, the stream function is zero on the boundary, $\psi_{|\partial\Omega} = 0$. The boundary conditions (2) translate into boundary conditions for the stream function

$$\left(-\frac{\partial \psi}{\partial y}, \frac{\partial \psi}{\partial x} \right) = \mathbf{u}_W(x, y, t), \quad (x, y) \in \partial\Omega. \tag{6}$$

There is no explicit boundary condition for the vorticity.

2.2. Matrix form of discretisation. The idea of the matrix formulation was initially introduced in Sousa and Sobey [13] for a one dimensional model problem which was similar to a stream-function vorticity problem and so included some of the features of that problem but in other respects was considerably simpler, having only two boundary points. In two dimensions we have a more complex problem for various reasons, one of them being the fact that we have a considerably larger number of points on the boundary.

As we have noted, the stream-function vorticity formulation has the advantage that it not only eliminates the pressure variable, but also automatically enforces incompressibility. Yet, a difficulty in the numerical simulation of (3) – (6) is deciding a suitable numerical boundary condition for the vorticity. When the vorticity advection-diffusion equation is updated in time, that does not provide values for the vorticity on the boundaries, only at mesh points in the interior of Ω so that an additional condition is needed to determine the vorticity on the boundary.

We will describe how the problem (3) – (6) is implemented in matrix form. We assume that we are in a cavity, with $\Omega = [0, 1] \times [0, 1]$ but these ideas generalise straight forwardly to arbitrary domains and to more complicated flows with inlet and outlet conditions.

We start by writing the discretised vorticity values in two vectors, $\mathbf{W}_I$, containing points which lie in the interior and $\mathbf{W}_B$ containing points on the boundary. The discrete values of the stream-function are similarly contained

in $\mathbf{\Psi}_I$, for the interior and $\mathbf{\Psi}_B$ for the boundary. A time update of the vorticity advection-diffusion equation provides an update for the interior vorticity values only. A fairly broad class of time marching discretisation for the vorticity advection equation, (3), can be written in the form

$$\mathbf{Q}\mathbf{W}_I^{n+1} = \mathbf{A}\mathbf{W}_I^n + \mathbf{B}\mathbf{W}_B^n, \tag{7}$$

for suitable matrices $\mathbf{Q}$, $\mathbf{A}$ and $\mathbf{B}$. Note that this formulation hides some aspects of the Navier-Stokes equations since according to (4), the matrices $\mathbf{A}$ and $\mathbf{B}$ are both functions of the stream-function, and thus implicitly of the vorticity. The equation (7), covers some implicit and all explicit time marching schemes. For these cavity problems, assume there is uniform discretization where the space step is the same in both directions, namely h, and that the mesh points are:

$$\{(jh, kh) : j, k = 0, \ldots, m\}.$$

Thus the vector $\mathbf{W}_I$ holds $(m-1)^2$ values and the vector $\mathbf{W}_B$ has $4m$ values. The dimensions of the matrices $\mathbf{Q}$ and $\mathbf{A}$ are $(m-1)^2 \times (m-1)^2$ and of the matrix $\mathbf{B}$ are $(m-1)^2 \times 4m$.

For a driven cavity flow, the natural ordering of the stream-function values implies an ordering of values $\psi_{jk} = \psi(jh, kh),\ j, k = 0, \ldots, m$ with $h = 1/m$. Suppose we denote a vector of values Ψ_{jk} which approximate ψ_{jk} using this natural ordering

$$\mathbf{\Psi} = [\Psi_{00}, \Psi_{10}, \Psi_{20}, \ldots, \Psi_{mm}]^T, \tag{8}$$

then there will exist a permutation matrix $\mathbf{P}$ such that

$$\mathbf{\Psi} = \mathbf{P} \begin{bmatrix} \mathbf{\Psi}_B \\ \mathbf{\Psi}_I \end{bmatrix}, \tag{9}$$

where $\mathbf{\Psi}_B$ are values on the boundary (j or k equal to 0 or m, in this case $4m$ values), $\mathbf{\Psi}_I$ those values in the interior ($0 < j, k < m$, in this case $(m-1)^2$ values) and if $\mathbf{P}$ is suitable partitioned as $\mathbf{P} = [\mathbf{P}_1, \mathbf{P}_2]$ then

$$\mathbf{\Psi} = \mathbf{P}_1\mathbf{\Psi}_B + \mathbf{P}_2\mathbf{\Psi}_I, \tag{10}$$

where the matrix $\mathbf{P}_1$ is a $(m+1)^2 \times 4m$ matrix and $\mathbf{P}_2$ is a $(m+1)^2 \times (m-1)^2$ matrix.

In a similar manner the vorticity approximation W_{jk}, can be written (using the same permutation matrices)

$$\mathbf{W} = [W_{00}, W_{10}, W_{20}, \ldots, W_{mm}]^T = \mathbf{P}_1\mathbf{W}_B + \mathbf{P}_2\mathbf{W}_I. \tag{11}$$

Next, the stream-function vorticity Poisson equation can be discretised at the interior points by

$$\mathbf{R}\boldsymbol{\Psi} = -h^2\mathbf{W}_I, \tag{12}$$

where $\mathbf{R}$ is a matrix of dimension $(m-1)^2 \times (m+1)^2$ and is easy to write down in terms of the natural ordering of $\boldsymbol{\Psi}$, so that in equation (12),

$$\frac{1}{h^2}\mathbf{L}\boldsymbol{\Psi}_I^{n+1} + \frac{1}{h^2}\mathbf{N}\boldsymbol{\Psi}_B^{n+1} = -\mathbf{W}_I^{n+1}, \tag{13}$$

$$\mathbf{L} = \mathbf{R}\mathbf{P}_2 \quad \text{and} \quad \mathbf{N} = \mathbf{R}\mathbf{P}_1. \tag{14}$$

and $\mathbf{L}$ is a $(m-1)^2 \times (m-1)^2$ and $\mathbf{N}$ is an $(m-1)^2 \times 4m$ matrix.

If the vorticity equation is discretised at the interior points (again using the natural ordering of $\boldsymbol{\Psi}^n$),

$$\mathbf{Q}\mathbf{W}_I^{n+1} = \mathbf{G}\mathbf{W}^n = \mathbf{G}[\mathbf{P}_1\mathbf{W}_B^n + \mathbf{P}_2\mathbf{W}_I^n], \tag{15}$$

where $\mathbf{G}$ is a matrix of dimensions $(m-1)^2 \times (m+1)^2$. Then

$$\mathbf{Q}\mathbf{W}_I^{n+1} = \mathbf{G}\mathbf{P}_1\mathbf{W}_B^n + \mathbf{G}\mathbf{P}_2\mathbf{W}_I^n, \tag{16}$$

so that the matrix $\mathbf{A}$ and $\mathbf{B}$ in (7) are determined by

$$\mathbf{A} = \mathbf{G}\mathbf{P}_2 \quad \text{and} \quad \mathbf{B} = \mathbf{G}\mathbf{P}_1. \tag{17}$$

The boundary vorticity is more complicated, since the discretisation there relates the wall vorticity to the updates stream-function, but if we use a natural ordering to obtain on the boundary

$$\mathbf{D}_1\mathbf{W}^{n+1} = \frac{1}{h^2}\mathbf{D}_2\boldsymbol{\Psi}^{n+1} + \mathbf{v}^{n+1}, \tag{18}$$

where $\mathbf{D_1}$ and $\mathbf{D_2}$ are $4m \times (m+1)^2$ matrices. The vector $\mathbf{v}^{n+1}$ might for instance arise in a driven cavity problem where the walls are moving. It follows that

$$\mathbf{D}_1[\mathbf{P}_1\mathbf{W}_B^{n+1} + \mathbf{P}_2\mathbf{W}_I^{n+1}] = \frac{1}{h^2}\mathbf{D}_2[\mathbf{P}_1\boldsymbol{\Psi}_B^{n+1} + \mathbf{P}_2\boldsymbol{\Psi}_I^{n+1}] + \mathbf{v}^{n+1}, \tag{19}$$

and so

$$\mathbf{D}_1\mathbf{P}_1\mathbf{W}_B^{n+1} = \frac{1}{h^2}\mathbf{D}_2\mathbf{P}_1\boldsymbol{\Psi}_B^{n+1} + \frac{1}{h^2}\mathbf{D}_2\mathbf{P}_2\boldsymbol{\Psi}_I^{n+1} - \mathbf{D}_1\mathbf{P}_2\mathbf{W}_I^{n+1} + \mathbf{v}^{n+1}. \tag{20}$$

This can be rewritten

$$\mathbf{W}_B^{n+1} = \frac{1}{h^2}\mathbf{M}\boldsymbol{\Psi}_I^{n+1} + \mathbf{F}\mathbf{W}_I^{n+1} + \frac{1}{h^2}\mathbf{J}\boldsymbol{\Psi}_B^{n+1} + (\mathbf{D}_1\mathbf{P}_1)^{-1}\mathbf{v}^{n+1}, \tag{21}$$

where the matrices $\mathbf{M}$, $\mathbf{F}$ and $\mathbf{J}$ are of dimensions $4m \times (m-1)^2$ and given by

$$\mathbf{M} = (\mathbf{D}_1\mathbf{P}_1)^{-1}\mathbf{D}_2\mathbf{P}_2, \quad \mathbf{F} = -(\mathbf{D}_1\mathbf{P}_1)^{-1}\mathbf{D}_1\mathbf{P}_2, \quad \mathbf{J} = (\mathbf{D}_1\mathbf{P}_1)^{-1}\mathbf{D}_2\mathbf{P}_1. \tag{22}$$

This enables the stream-function to be eliminated in the interior using (13)

$$\mathbf{W}_B^{n+1} = (\mathbf{F} - \mathbf{M}\mathbf{L}^{-1})\mathbf{W}_I^{n+1} + \frac{1}{h^2}(\mathbf{J} - \mathbf{M}\mathbf{L}^{-1}\mathbf{N})\mathbf{\Psi}_B^{n+1} + (\mathbf{D}_1\mathbf{P}_1)^{-1}\mathbf{v}^{n+1}, \tag{23}$$

and then the update of the vorticity in the interior can be replaced so that

$$\mathbf{W}_B^{n+1} = (\mathbf{F} - \mathbf{M}\mathbf{L}^{-1})\mathbf{Q}^{-1}(\mathbf{A}\mathbf{W}_I^{n} + \mathbf{B}\mathbf{W}_B^{n}) + \frac{1}{h^2}(\mathbf{J} - \mathbf{M}\mathbf{L}^{-1}\mathbf{N})\mathbf{\Psi}_B^{n+1} + (\mathbf{D}_1\mathbf{P}_1)^{-1}\mathbf{v}^{n+1}. \tag{24}$$

This essentially completes the derivation of the iteration matrix for this version of the Navier-Stokes equations, since we now have

$$\begin{bmatrix} \mathbf{W}_I^{n+1} \\ \mathbf{W}_B^{n+1} \end{bmatrix} = \begin{bmatrix} \mathbf{Q}^{-1}\mathbf{A} & \mathbf{Q}^{-1}\mathbf{B} \\ (\mathbf{F} - \mathbf{M}\mathbf{L}^{-1})\mathbf{Q}^{-1}\mathbf{A} & (\mathbf{F} - \mathbf{M}\mathbf{L}^{-1})\mathbf{Q}^{-1}\mathbf{B} \end{bmatrix} \begin{bmatrix} \mathbf{W}_I^{n} \\ \mathbf{W}_B^{n} \end{bmatrix} + \mathbf{S}^{n+1}, \tag{25}$$

or

$$\mathbf{W}^{n+1} = \mathbf{K}\mathbf{W}^{n} + \mathbf{S}^{n+1}, \tag{26}$$

where

$$\mathbf{S}^{n+1} = \frac{1}{h^2}\begin{bmatrix} 0 \\ (\mathbf{J} - \mathbf{M}\mathbf{L}^{-1}\mathbf{N})\mathbf{\Psi}_B^{n+1} \end{bmatrix} + (\mathbf{D}_1\mathbf{P}_1)^{-1}\mathbf{v}^{n+1}$$

and $\mathbf{K}$ denotes the overall iteration matrix,

$$\mathbf{K} = \begin{bmatrix} \mathbf{Q}^{-1}\mathbf{A} & \mathbf{Q}^{-1}\mathbf{B} \\ (\mathbf{F} - \mathbf{M}\mathbf{L}^{-1})\mathbf{Q}^{-1}\mathbf{A} & (\mathbf{F} - \mathbf{M}\mathbf{L}^{-1})\mathbf{Q}^{-1}\mathbf{B} \end{bmatrix}. \tag{27}$$

Let $\mathbf{X} = \mathbf{F} - \mathbf{M}\mathbf{L}^{-1}$, $p = (m-1)^2$ and $q = 4m$. We have

$$\mathbf{K}_{(p+q)^2} = \begin{bmatrix} \mathbf{Q}^{-1}\mathbf{A}_{p\times p} & \mathbf{Q}^{-1}\mathbf{B}_{p\times q} \\ \mathbf{X}\mathbf{Q}^{-1}\mathbf{A}_{q\times p} & \mathbf{X}\mathbf{Q}^{-1}\mathbf{B}_{q\times q} \end{bmatrix},$$

and we can observe that

$$\mathbf{K} = \begin{bmatrix} \mathbf{I}_{p\times p} & \mathbf{0}_{p\times q} \\ \mathbf{X}_{q\times p} & \mathbf{I}_{q\times q} \end{bmatrix} \begin{bmatrix} \mathbf{Q}^{-1}_{p\times p} & \mathbf{0}_{p\times q} \\ \mathbf{0}_{q\times p} & \mathbf{I}_{q\times q} \end{bmatrix} \begin{bmatrix} \mathbf{A}_{p\times p} & \mathbf{B}_{p\times q} \\ \mathbf{0}_{q\times p} & \mathbf{0}_{q\times q} \end{bmatrix}.$$

Note that if we have an explicit scheme then $\mathbf{Q} = \mathbf{I}$ so that

$$\mathbf{K} = \begin{bmatrix} \mathbf{I} & \mathbf{0} \\ \mathbf{X} & \mathbf{I} \end{bmatrix} \begin{bmatrix} \mathbf{A} & \mathbf{B} \\ \mathbf{0} & \mathbf{0} \end{bmatrix} \tag{28}$$

and $\mathbf{X}$ represents the influence of the vorticity boundary conditions and Poisson's equation and $\mathbf{A}$ and $\mathbf{B}$ the influence of the vorticity equation.

In this work we consider two-level time-integration schemes and constant boundary conditions so that $\mathbf{S}^{n+1} = \mathbf{S}$, is constant and so,

$$\mathbf{W}^{n+1} = \mathbf{K_n}\mathbf{W}^n + \mathbf{S}, \tag{29}$$

where $\mathbf{S}$ contains boundary values of the stream-function and of the velocity field and in the case where the flow field is evolving or time dependent since then the global iteration matrix varies from iteration to iteration and so is denoted $\mathbf{K_n}$.

In section 4 below we consider a case where $\mathbf{K_n}$ is constant, $\mathbf{K_n} = \mathbf{K}$. Since the flow field is constant and known in advance,

$$\mathbf{W}^{n+1} = \mathbf{K}\mathbf{W}^n + \mathbf{S}. \tag{30}$$

For such a steady flow, we can denote the difference between the steady solution, $\mathbf{W}$ and the current iteration value, $\mathbf{W}^n$ as an error, $\mathbf{e}^n = \mathbf{W} - \mathbf{W}^n$.

In that case the error $\mathbf{e}^n$ satisfies the equation

$$\mathbf{e}^{n+1} = \mathbf{K}\mathbf{e}^n = \mathbf{K}^{n+1}\mathbf{e}^0. \tag{31}$$

When $\mathbf{K}$ is constant, we have the following stability condition, see Richtmyer and Morton [14].

Stability condition: In order for $\mathbf{W}^n$ to remain bounded and the scheme, defined by the operator $\mathbf{K}^{n+1}$, to remain stable, the infinite set of operators $\mathbf{K}^n$ has to be uniformly bounded. That is, we should have, in a selected norm, for finite T

$$||\mathbf{K}^n|| < C \text{ for } 0 < n\Delta t < T,$$

where C is independent of $n, \Delta t, h$.

The norm of $\mathbf{K}^n$ is often very difficult to analyse, and instead a necessary condition but not always sufficient condition can be obtained from an analysis of the eigenvalues of $\mathbf{K}$.

The condition $\rho(\mathbf{K}) \leq 1$ is necessary for the scheme implemented by (30) to be stable, where $\rho(\mathbf{K})$ is the spectral radius of $\mathbf{K}$.

We have the following result.

Proposition 1: The value $\lambda \neq 0$ is an eigenvalue of the matrix $\mathbf{K}$, defined by (28), if and only if is an eigenvalue of the matrix $\mathbf{A} + \mathbf{BX}$.

Proof: If $\lambda \neq 0$ is an eigenvalue of the matrix $\mathbf{K}$ then exists $\mathbf{z}$ such that $\mathbf{Kz} = \lambda\mathbf{z}$. From this, we get $\mathbf{Az_1} + \mathbf{Bz_2} = \lambda\mathbf{z_1}$ and $\mathbf{XAz_1} + \mathbf{XBz_2} = \lambda\mathbf{z_2}$,

where $\mathbf{z} = [\mathbf{z_1}\ \mathbf{z_2}]^T$. We have $\mathbf{Xz_1} = \mathbf{z_2}$ and then $\mathbf{Az_1} + \mathbf{BXz_1} = \lambda\mathbf{z_1}$ and λ is an eigenvalue of $\mathbf{A} + \mathbf{BX}$.

Reciprocally if λ is an eigenvalue of $\mathbf{A} + \mathbf{BX}$ then there is $\mathbf{z_1}$ such that $\mathbf{Az_1} + \mathbf{BXz_1} = \lambda\mathbf{z_1}$. Therefore λ is an eigenvalue of $\mathbf{K}$, since we have $\mathbf{Kz} = \lambda\mathbf{z}$, where $\mathbf{z} = [\mathbf{z_1}\ \mathbf{Xz_1}]^T$.

We can not easily get explicit conditions between the eigenvalues of $\mathbf{A}$ and the eigenvalues of $\mathbf{A} + \mathbf{BX}$, since neither $\mathbf{A}$ or $\mathbf{BX}$ are special matrices, namely symmetric or other. However the fact that the eigenvalues of $\mathbf{K}$ are the eigenvalues of $\mathbf{A} + \mathbf{BX}$ shows us more clearly that the different choices of the vorticity boundary conditions, implicitly represented by $\mathbf{X}$, can affect the spectral radius of $\mathbf{K}$.

Also if we want to compute numerically the spectrum of $\mathbf{K}$ for large dimensions is more efficient to use the matrix $\mathbf{A} + \mathbf{BX}$.

In later sections we are also going to use a fourth-order Poisson discretisation. Briefly, we point out the changes that occurs in the matrix formulation when using this discretisation.

The formula (13) come as

$$\frac{1}{h^2}\mathbf{L}\boldsymbol{\Psi}_I^{n+1} + \frac{1}{h^2}\mathbf{N}\boldsymbol{\Psi}_B^{n+1} = -\mathbf{T_1}\mathbf{W}_I^{n+1} - \mathbf{T_2}\mathbf{W}_B^n, \tag{32}$$

and then

$$\boldsymbol{\Psi}_I^{n+1} = -\mathbf{L}^{-1}\mathbf{N}\boldsymbol{\Psi}_B^{n+1} - h^2\mathbf{L}^{-1}\mathbf{T_1}\mathbf{W}_I^{n+1} - h^2\mathbf{L}^{-1}\mathbf{T_2}\mathbf{W}_B^n. \tag{33}$$

Consequently (23) is now given by

$$\mathbf{W}_B^{n+1} = (\mathbf{F}-\mathbf{M}\mathbf{L}^{-1}\mathbf{T_1})\mathbf{W}_I^{n+1} - \mathbf{M}\mathbf{L}^{-1}\mathbf{T_2}\mathbf{W}_B^n + \frac{1}{h^2}(\mathbf{J}-\mathbf{M}\mathbf{L}^{-1}\mathbf{N})\boldsymbol{\Psi}_B^{n+1} + (\mathbf{D}_1\mathbf{P}_1)^{-1}\mathbf{v}^{n+1}, \tag{34}$$

and then

$$\mathbf{W}_B^{n+1} = \left[(\mathbf{F}-\mathbf{M}\mathbf{L}^{-1}\mathbf{T_1})\mathbf{Q}^{-1}\mathbf{A} \qquad (\mathbf{F}-\mathbf{M}\mathbf{L}^{-1}\mathbf{T_1})\mathbf{Q}^{-1}\mathbf{B} - \mathbf{M}\mathbf{L}^{-1}\mathbf{T_2}\right] \begin{bmatrix} \mathbf{W}_I^n \\ \mathbf{W}_B^n \end{bmatrix} + \mathbf{S}^{n+1}. \tag{35}$$

3. Finite difference discretisations

In this section we set out two different schemes for the unsteady vorticity advection-diffusion equation; one a second order Lax–Wendroff type scheme and one a third order, Quickest type scheme. These schemes, which are forms of well known schemes of the same name, were introduced in Sousa

and Sobey [15]. We consider two schemes for discretising a Poisson equation, one the usual second order central difference scheme and one a fourth order scheme (see Iserles [16]). We also set out a number of well known schemes for discretising the boundary vorticity, that of Thom [2], Woods [17], Jensen [18], d'Alessio and Dennis [19] and Briley [20]. We note in passing some consequences for stability from the discretisation of the advection-diffusion equation.

3.1. Discretisation of the vorticity advection-diffusion equation. We use the difference operators,

$$\Delta_{x0}W_{j,k} = \frac{1}{2}(W_{j+1,k} - W_{j-1,k}),$$

$$\delta_x^2 W_{j,k} = W_{j+1,k} - 2W_{j,k} + W_{j-1,k},$$

$$\Delta_{x-}W_{j,k} = W_{j,k} - W_{j-1,k}$$

with operators $\Delta_{y0}W_{j,k}, \delta_y^2 W_{j,k}, \Delta_{y-}W_{j,k}$ defined analogously.

Also define local numerical parameters,

$$\nu_x = \frac{u\Delta t}{h}, \qquad \nu_y = \frac{v\Delta t}{h}, \qquad \mu = \frac{1}{Re}\frac{\Delta t}{h^2},$$

where Δt is the time-step so that the iteration time is $t_n = n\Delta t$.

We discretise the vorticity advection-diffusion equation (3) on the $(m-1)\times(m-1)$ interior points using two different numerical schemes.

An explicit second-order numerical Lax-Wendroff type scheme is given by:

$$\begin{aligned} W_{jk}^{n+1} &= W_{jk}^n - \nu_x\Delta_{x0}W_{jk}^n + (\frac{1}{2}\nu_x^2 + \mu_x)\delta_x^2 W_{jk}^n - \nu_y\Delta_{y0}W_{jk}^n \\ &\quad +(\frac{1}{2}\nu_y^2 + \mu_y)\delta_y^2 W_{jk}^n + \nu_x\nu_y\Delta_{x0}\Delta_{y0}W_{jk}^n,\ j,k = 1,\ldots,m-1. \end{aligned} \tag{36}$$

This scheme uses a nine point stencil and can be used independently of the direction of the velocity field (u, v).

An explicit third-order Quickest type scheme is given by:

$$\begin{aligned} W_{jk}^{n+1} &= W_{jk}^n - \nu_x\Delta_{x0}W_{jk}^n - \nu_y\Delta_{y0}W_{jk}^n + (\frac{1}{2}\nu_x^2 + \mu_x)\delta_x^2 W_{jk}^n \\ &\quad +(\frac{1}{2}\nu_y^2 + \mu_y)\delta_y^2 W_{jk}^n + \nu_x\nu_y\Delta_{x0}\Delta_{y0}W_{jk}^n \\ &\quad +\frac{1}{6}\nu_x(1-\nu_x^2-6\mu_x)\delta\Delta_x W_{jk}^n + \frac{1}{6}\nu_y(1-\nu_y^2-6\mu_y)\delta\Delta_y W_{jk}^n \end{aligned}$$

$$-\nu_y(\mu_x + \frac{1}{2}\nu_x^2)\delta_x^2\Delta_{y0}W_{jk}^n - \nu_x(\mu_y + \frac{1}{2}\nu_y^2)\delta_y^2\Delta_{x0}W_{jk}^n,$$
$$j,k = 1,\ldots,m-1, \tag{37}$$

where the operators $\delta\Delta_x$ and $\delta\Delta_y$ change according to the direction of the velocity field as described in the table below. This scheme uses an eleven point stencil.

	$u,v \geq 0$	$u \geq 0, v \leq 0$	$u \leq 0, v \geq 0$	$u,v \leq 0$
$\delta\Delta_x$	$\delta_x^2\Delta_{x-}$	$\delta_x^2\Delta_{x-}$	$\delta_x^2\Delta_{x+}$	$\delta_x^2\Delta_{x+}$
$\delta\Delta_y$	$\delta_y^2\Delta_{y-}$	$\delta_y^2\Delta_{y+}$	$\delta_y^2\Delta_{y-}$	$\delta_y^2\Delta_{y+}$

Definition of the operators $\delta\Delta_x$ and $\delta\Delta_y$.

In the case of a non-linear velocity field, we treat these difference expansions as local approximations and use the velocity components (u,v) involved in the variables ν_x and ν_y at the central mesh point, (x_j, y_k). For additional information on the derivation of these two schemes see Sousa and Sobey [15].

If we retain the locally constant approximation then the stability of the iteration is from a linear problem and we can use von Neumann stability analysis for the Cauchy problem involving the advection-diffusion vorticity equation. This gives us necessary conditions for stability which are usually worthwhile taking into consideration in the non-linear problem.

A von Neumann analysis in two dimensions is a straightforward generalisation of the one-dimensional case. The discrete Fourier decomposition in two dimensions consists of the decomposition of the function into a Fourier series as

$$U_{jk}^n = \sum_{\xi_x,\xi_y} \kappa^n \mathrm{e}^{\mathrm{i}\xi_x j\Delta x}\mathrm{e}^{\mathrm{i}\xi_y k\Delta y},$$

where the range ξ_x, ξ_y is defined separately for each direction, as in the one-dimensional case. The amplification factor is given by κ. The products $\xi_x\Delta x$ and $\xi_y\Delta y$ are often represented as a phase angle, namely, $\theta_x = \xi_x\Delta x$, $\theta_y = \xi_y\Delta y$. To obtain a von Neumann stability condition we insert the singular component $\kappa^n\mathrm{e}^{\mathrm{i}j\theta_x}\mathrm{e}^{\mathrm{i}k\theta_y}$ into the discretised scheme. The amplification factor is said to satisfy the von Neumann condition if there is a constant K such that

$$|\kappa(\theta_x,\theta_y)| \leq 1 + K\Delta t \quad \forall\ \theta_x,\theta_y \in [0,2\pi]. \tag{38}$$

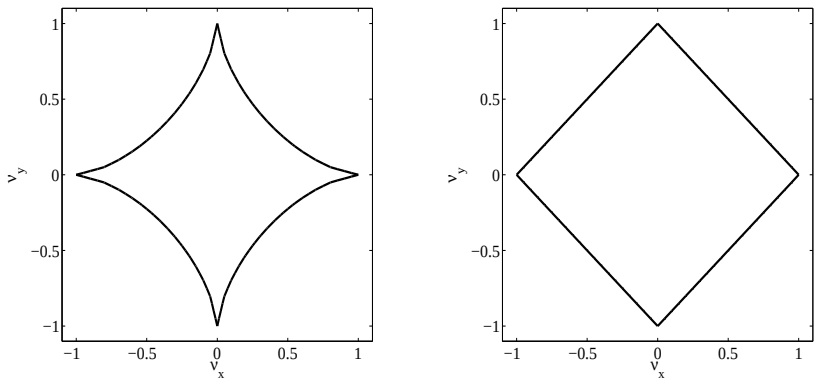

(a) (b)

FIGURE 1. Stability conditions given in Proposition 2: (a) Second-order scheme. (b) Third-order scheme.

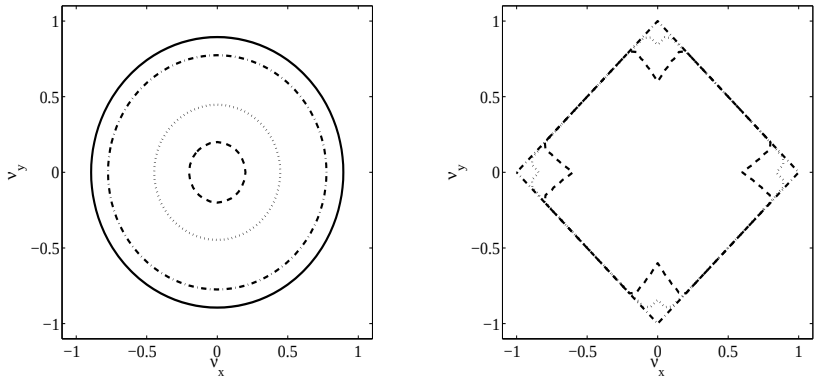

(a) (b)

FIGURE 2. Stability conditions given in Proposition 3: (a) Second-order scheme: contours for $\mu = 0.05$ $(-)$; $\mu = 0.1$ $(- \cdot -)$; $\mu = 0.2$ $(\cdots)$; $\mu = 0.24$ $(--)$. (b) Third-order scheme: contours for $\mu = 0.1$ $(-\cdot-)$; $\mu = 0.2$ $(\cdots)$; $\mu = 0.24$ $(--)$.

As in the one-dimensional case, in practice we use the stronger condition

$$|\kappa(\theta_x, \theta_y)| \leq 1 \quad \forall\ \theta_x, \theta_y \in [0, 2\pi], \tag{39}$$

and the discrete scheme that meets this condition, we refer to as von Neumann stable. This has been called practical stability by Richtmyer and Morton [14] or strict stability by other authors. In some cases condition (38) allows numerical modes to grow exponentially in time for finite values of Δt. Therefore, the practical, or strict, stability condition (39) is recommended in order to prevent numerical modes from growing faster than the physical modes of the differential equation.

For our finite difference schemes we have the following results, that are also represented in Figures 1 and 2.

Proposition 2: For the hyperbolic problem, that is, $\mu = 0$, we have:
(a) The scheme (36) is stable if and only if

$$|\nu_x|^{2/3} + |\nu_y|^{2/3} \leq 1. \tag{40}$$

(b) The scheme (37) is stable only if

$$|\nu_x| + |\nu_y| \leq 1. \tag{41}$$

Proof:
(a) This is well known, see Turkel [21].
(b) Let $u, v \geq 0$ so that $\nu_x, \nu_y \geq 0$. The amplification factor for the phase angles $\theta_x = 0$ and $\theta_y = \pi$ gives that to have $|\kappa| \leq 1$ is the same as to have $\nu_x \leq 1$. Similarly for the phase angles $\theta_x = \pi$ and $\theta_y = 0$, we have $\nu_y \leq 1$.Then assuming $\nu_x, \nu_y \leq 1$ for the phase angles of high frequency $\theta_x = \theta_y = \pi$, $|\kappa| \leq 1$ is equivalent to $\nu_x + \nu_y \leq 1$. Similarly results could be obtained for different directions of the velocity field in order to obtain condition (41).

Proposition 3:
(a) Necessary von Neumann conditions for the stability of the scheme (36) are

$$4\mu \leq 1 \qquad \nu_x^2 + \nu_y^2 \leq 1 - 4\mu.$$

(b) A necessary von Neumann condition for the stability of the scheme (37) is

$$(\nu_x^2 + 2\mu) + (\nu_y^2 + 2\mu) + \frac{2}{3}|\nu_x|(1 - \nu_x^2 - 6\mu) + \frac{2}{3}|\nu_y|(1 - \nu_y^2 - 6\mu) \leq 1.$$

Proof:
(a) The first condition is obtained in the limiting case $\theta_x \to 0$, $\theta_y \to 0$. The second condition is obtained from the particular case $\theta_x = \theta_y = \pi$.
(b) Let $u, v \geq 0$ so that $\nu_x, \nu_y \geq 0$. The second condition is obtained from the particular case $\theta_x = \theta_y = \pi$.

3.2. Discretisation of the Poisson equation. We consider two discretisations of the Poisson equation, (5). The first is the usual second order central

difference scheme,

$$(\delta_x^2 + \delta_y^2)\Psi_{j,k}^{n+1} = -h^2 W_{j,k}^{n+1}. \tag{42}$$

The second discretisation was originated by Collatz [22], see also Iserles [16],

$$(\delta_x^2 + \delta_y^2 + \frac{1}{6}\delta_x^2\delta_y^2)\Psi_{j,k}^{n+1} = -h^2(I + \frac{1}{12}(\delta_x^2 + \delta_y^2))W_{j,k}^{n+1} \tag{43}$$

where I is an identity operator. This scheme is fourth order accurate in h. We believe that this scheme is the same as that advocated in Spotz [12] who derived the scheme afresh using discrete approximation for high order derivatives in the truncation error.

3.3. Boundary vorticity discretisation. While there are no formal or explicit conditions on the vorticity at a wall, it is necessary to use an implicit condition in order to provide the vorticity at the wall. There are various different methods for specifying wall vorticity, $\mathbf{W}_B$, in terms of the vorticity in the interior and the stream function. An extensive review of methods for dealing with the boundary vorticity can be found in Napolitano et al. [10]. In terms of our matrix formulation, different boundary vorticity schemes imply changes only in the matrices $\mathbf{D}_1, \mathbf{D}_2$.

The conditions we use to calculate the vorticity on the boundaries are illustrated for one boundary, $y = 0$. Since the velocity field on that boundary, $u(x, 0)$, is not zero, the formulae assume that $\psi_y = u$ implicitly on the boundary. The formulae below are due to Thom [2], Woods [17], Jensen [18], d'Alessio and Dennis [19] and Briley [20].

$$\textbf{Thom:} \qquad W_{j0} = \frac{2}{h^2}(\Psi_{j0} - \Psi_{j1} + hu(jh, 0)) \tag{44}$$

$$\textbf{Woods:} \qquad W_{j0} = \frac{3}{h^2}(\Psi_{j0} - \Psi_{j1} + hu(jh, 0)) - \frac{1}{2}W_{j1} \tag{45}$$

$$\textbf{Jensen:} \qquad W_{j0} = \frac{1}{2h^2}(7\Psi_{j0} - 8\Psi_{j,1} + \Psi_{j2} + 6hu(jh, 0)) \tag{46}$$

$$\textbf{D'Alessio \& Dennis:} \quad W_{j0} = \frac{4}{h^2}(\Psi_{j0} - \Psi_{j1} + hu(jh, 0)) - \frac{1}{3}(4W_{j1} - W_{j2}) \tag{47}$$

$$\textbf{Briley:} \quad W_{j0} = \frac{1}{18h^2}(85\Psi_{j,0} - 108\Psi_{j,1} + 27\Psi_{j,2} - 4\Psi_{j,3} + 66hu(jh, 0)). \tag{48}$$

We omit the superscript $n + 1$ defining the time, t_{n+1}, in the formulas (44)-(48), all the variables are taken at the updated time level, t_{n+1}. The discretisation for the other boundaries is analogous. Considering (18) we have

for Thom's vorticity boundary condition that $\mathbf{D}_1 = \mathbf{I}$ where $\mathbf{I}$ is the matrix identity, and $\mathbf{D}_2$ depends of the values of Ψ at the boundary discretisation. For Woods' and d'Allesio & Dennis' boundary condition $\mathbf{D}_1$ is no longer an identity matrix. Also for Thom's, Jensen's and Briley's formulae, $\mathbf{F} = \mathbf{0}$, since they do not depend of the interior vorticity values. The order of accuracy of the various methods (see Napolitano et al. [10]) is $O(h)$ for Thom's, $O(h^2)$ for Woods', Jensen's and d'Alessio & Dennis' and $O(h^3)$ for Briley's.

4. Cavity flow which is exact solution of Navier–Stokes equations

In this section we approach the problem of using the global iteration matrix by turning to an exact solution of the Navier–Stokes equations. The solution is somewhat contrived in that it relies on a body force which may not be attainable in reality but it is, nevertheless, an exact solution and thus allows consideration of precisely defined error measures, whereas normally in dealing with flow problems, one can only test against solutions obtained from refined meshes.

We start from the stream-function

$$\psi(x, y) = \frac{1}{\pi} \sin \pi x \ \sin \pi y, \tag{49}$$

which will take constant (zero) value on the boundaries of the unit square and so in one sense can be described as a driven cavity problem. This stream-function describes a flow with velocity field $\mathbf{u} = (u, v)$

$$u(x, y) = \sin \pi x \ \cos \pi y, \tag{50}$$

$$v(x, y) = -\cos \pi x \ \sin \pi y, \tag{51}$$

and vorticity

$$\omega = -\nabla^2 \psi = 2\pi \sin \pi x \ \sin \pi y. \tag{52}$$

In order to make this an exact solution, consider the momentum equation in the Navier-Stokes equations, (1), with the addition of a body force, $\mathbf{f}$,

$$\frac{\partial \mathbf{u}}{\partial t} + (\mathbf{u} \cdot \nabla)\mathbf{u} = -\nabla p + \frac{1}{Re} \nabla^2 \mathbf{u} + \mathbf{f}, \tag{53}$$

and choose

$$p = \frac{1}{4}(\cos 2\pi x + \cos 2\pi y), \tag{54}$$

$$\mathbf{f} = \frac{2\pi^2}{Re}[\sin \pi x \ \cos \pi y, -\cos \pi x \ \sin \pi y]. \tag{55}$$

The set ψ, p and $\mathbf{f}$ provide an **exact** solution to the **steady** Navier-Stokes equations.

The problem we consider is to suppose that we have some distribution of vorticity $W(x, y, t)$ and stream-function, $\Psi(x, y, t)$ related by

$$\nabla^2 \Psi = -W, \tag{56}$$

but subject to the steady velocity field $\mathbf{u}$ and body force $\mathbf{f}$ through the vorticity advection equation which results from (53). The time dependent Navier-Stokes equations will give $W \to \omega$ as $t \to \infty$ and we let W satisfy:

$$\frac{\partial W}{\partial t} + (\mathbf{u} \cdot \nabla) W = \frac{1}{Re} \nabla^2 W - \frac{1}{Re} \nabla^2 \omega. \tag{57}$$

Now use the result that *for this exact steady flow field*

$$\frac{\partial \omega}{\partial t} \equiv 0, \quad (\mathbf{u} \cdot \nabla) \omega \equiv 0, \tag{58}$$

so that the difference, $e = W - \omega$, satisfies

$$\frac{\partial e}{\partial t} + (\mathbf{u} \cdot \nabla) e = \frac{1}{Re} \nabla^2 e. \tag{59}$$

We interpret e as an error in a vorticity field, the error satisfying an advection diffusion equation with a velocity field which is spatially varying but constant in time. If the vorticity time variation on the boundary is set to zero, then the vorticity error will decay to zero in time as $W \to \omega$ and properties of the discretisation of the advection-diffusion equation alone should determine the vorticity time variation behavior in time. If, however, the boundary vorticity is not specified explicitly, but determined as usual for the stream-function vorticity formulation, then the error will not decay to zero in time but will reflect a **global** truncation error of the discretisation of the whole stream-function vorticity system. Hence the procedure to carry out one time step is: (a) update the error e in the interior of the domain using (59), (b) calculate W in the interior from $W = e + \omega$, (c) calculate the stream-function, Ψ in the interior by solving $\nabla^2 \Psi = -W$, (d) calculate the vorticity W on the boundary using an appropriate method, and finally (e) calculate the error on the boundary using $e = W - \omega$.

There are two numerical parameters which characterise the system,

$$\nu = \frac{\Delta t}{h} \qquad \mu = \frac{1}{Re} \frac{\Delta t}{h^2}.$$

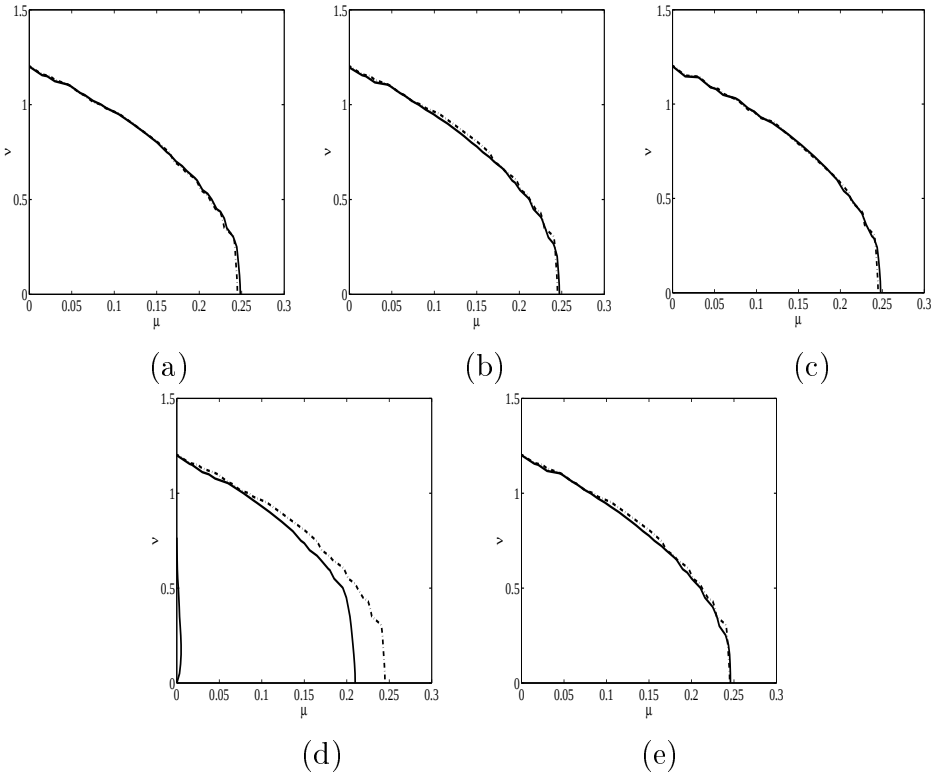

FIGURE 3. Eigenvalues less than one: The local matrix A $(\cdot-)$; the global matrix K $(-)$; $m = 32$. Second-order method for advection-diffusion with: (a) Thom's boundary condition; (b) Woods's boundary condition; (c) Jensen boundary condition; (d) Alessio's boundary condition; (e) Briley's boundary condition.

4.1. Stability. We consider consequences for stability of choosing different boundary vorticity conditions. Since the vorticity difference, e, satisfies an advection-diffusion equation with constant velocity field we can examine stability through the global iteration matrix, $\mathbf{K}$, defined in (27), where we used the second-order Poisson's discretisation.

The results for the eigenvalues of $\mathbf{K}$ for different vorticity boundary conditions with the second order Lax–Wendroff type scheme are shown in figure 3 where we also show the eigenvalues of the iteration matrix for the advection-diffusion equation, $\mathbf{A}$, The results were obtained for the mesh size $m = 32$. The overall pattern is that there may be a small reduction in the region of stability with higher order methods but in general, the choice of boundary vorticity discretisation does not have significant stability penalties. Mesh refinement does not affect this conclusion.

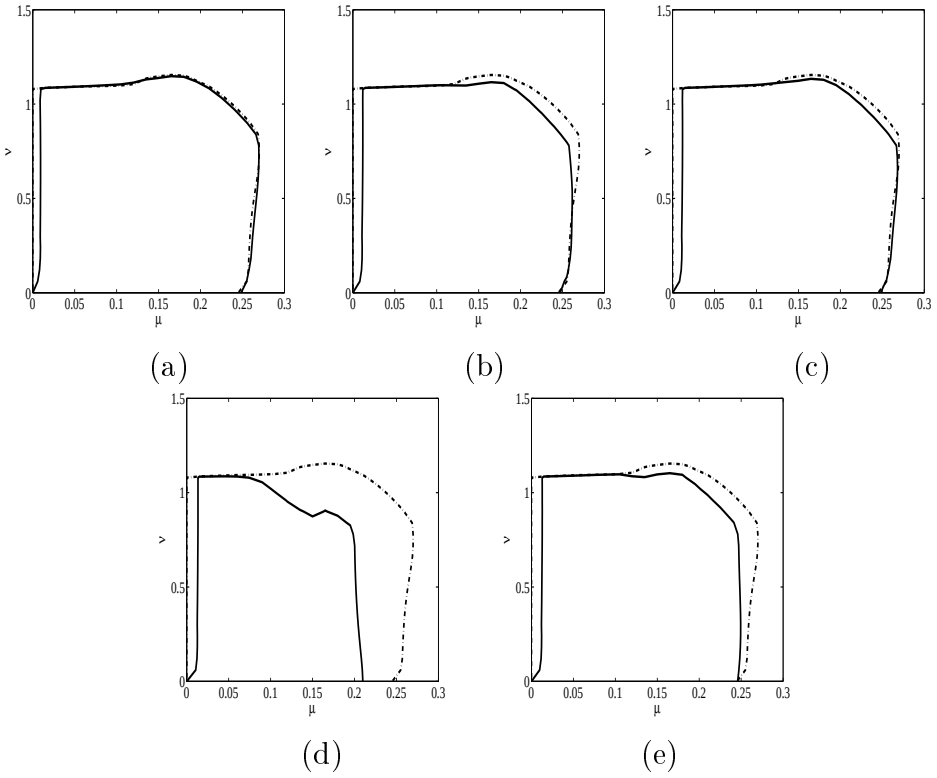

FIGURE 4. Eigenvalues less than one: The local matrix A $(\cdot-)$; the global matrix K $(-)$; $m = 32$. Third-order method for advection-diffusion with: (a) Thom's boundary condition; (b) Wood's boundary condition; (c) Jensen boundary condition; (d) Alessio's boundary condition; (e) Briley's boundary condition.

We have also considered the case of a third order Quickest type scheme for the advection-diffusion equation and the regions of stability are shown in figure 4. In this case there is a more noticeable stability penalty but again, only marginally important. There is a region near the $\mu = 0$ axis where the eigenvalues are predicted to be very slightly greater than one but in practical computations, the iterations remain stable in this region.

Although Figures 3 and 4 display the stability regions obtained when using the second-order Poisson's discretisation, for the fourth-order Poisson discretisation (43) we obtain very similar stability regions.

4.2. Accuracy. We have used solution of the system (56) and (59) to examine the accuracy of the different numerical schemes although as we shall see in the next section, the conclusions are more limited than we had hoped.

We start the iteration with the vorticity initially set to have unit value everywhere except at the four corner nodes where it is set to zero (the corner values of the vorticity are not used anywhere in the iteration). The system is then updated according to the scheme described above with the following possible choices:
i) Lax–Wendroff or Quickest for advection-diffusion equation,
ii) a second or fourth order scheme for solution of the Poisson equation,
iii) boundary vorticity scheme from: Thom, Woods, Jensen, d'Allessio & Dennis or Briley.

The Poisson equation was solved using a four-level multigrid solver with convergence criterion set to L_∞ norm of the residual less than 10^{-7}. As the global error is converging to zero as the mesh size vanishes, the order of convergence can be extrapolated using two meshes. In the results we do this for 16×16 and 32×32 meshes and for 32×32 and 64×64 meshes.

The results shown in table 1 are a little surprising since for the majority of cases second order convergence is obtained regardless of the discretisation of the vorticity equation or which form of boundary condition is used, however, in the case of Jensen or Briley's method, fourth order convergence is obtained when the Poisson solver is also fourth order. We believe that this is consistent with the theory of Bramble and Hubbard [23] who showed that for an elliptic problem with truncation error $O(h^n)$ [h is mesh spacing] then the global error would remain $O(h^n)$ when there were local errors of order $O(h^{n-1})$ near a boundary with a mixed or Neumann condition and $O(h^{n-2})$ near a boundary with Dirichlet condition. The complexity of this particular problem means that we cannot prove this result formally at present. It is also surprising that the discretisation of the vorticity equation does not affect the numerical results but that too may be consistent with the theory of Bramble and Hubbard [23] or it may be a consequence of the very artificial nature of this test problem. Since in the next section where we consider a driven cavity flow, we do not see this behavior, it is most likely that the convergence here is determined more by the solution of Poisson equation than by the solution of the advection diffusion equation so that the correct explanation for the global convergence rate comes from Bramble–Hubbard theory.

Boundary method	Convection Diffusion	Poisson Equation	Error			Convergence	
			16×16	32×32	64×64	16-32	32-64
Thom	Lax-Wendroff	$O(h^2)$	0.914E-02	0.222E-02	0.546E-03	2.04	2.02
		$O(h^4)$	0.181E-01	0.443E-02	0.109E-02	2.03	2.02
	Quickest	$O(h^2)$	0.909E-02	0.222E-02	0.546E-03	2.03	2.02
		$O(h^4)$	0.180E-01	0.443E-02	0.109E-02	2.02	2.02
Woods	Lax-Wendroff	$O(h^2)$	0.278E-01	0.668E-02	0.164E-02	2.06	2.03
		$O(h^4)$	0.183E-01	0.444E-02	0.109E-02	2.04	2.02
	Quickest	$O(h^2)$	0.275E-01	0.667E-02	0.164E-02	2.04	2.02
		$O(h^4)$	0.181E-01	0.444E-02	0.109E-02	2.03	2.02
Jensen	Lax-Wendroff	$O(h^2)$	0.925E-02	0.223E-02	0.546E-03	2.06	2.03
		$O(h^4)$	0.154E-03	0.930E-05	0.571E-06	4.05	4.03
	Quickest	$O(h^2)$	0.915E-02	0.222E-02	0.546E-03	2.04	2.03
		$O(h^4)$	0.153E-03	0.930E-05	0.571E-06	4.04	4.03
d'Allesio	Lax-Wendroff	$O(h^2)$	0.686E-01	0.137E-01	0.319E-02	2.32	2.11
		$O(h^4)$	0.611E-01	0.123E-01	0.284E-02	2.31	2.11
	Quickest	$O(h^2)$	0.653E-01	0.136E-01	0.318E-02	2.26	2.10
		$O(h^4)$	0.582E-01	0.122E-01	0.283E-02	2.26	2.10
Briley	Lax-Wendroff	$O(h^2)$	0.961E-02	0.224E-02	0.547E-03	2.10	2.04
		$O(h^4)$	0.103E-03	0.628E-05	0.387E-06	4.04	4.02
	Quickest	$O(h^2)$	0.947E-02	0.224E-02	0.547E-03	2.08	2.03
		$O(h^4)$	0.102E-03	0.627E-05	0.387E-06	4.02	4.02

Table 1. Global L_2 error of time converged solution for three mesh resolutions, 16×16, 32×32 and 64×64, with calculated convergence rate for varying vorticity boundary condition, convection-diffusion discretisation and discretisation of stream function-vorticity equation.
Numerical parameters are : $Re = 100$, $\Delta t = 0.0005$, multigrid residual less than 10^{-7}.

5. Driven cavity laminar flow

In the this section we consider time marching solutions for a full Navier-Stokes problem using the range of discretisations just described and present stability regions and some numerical results for accuracy. This problem has long served as the prototype for the incompressible Navier-Stokes equations; see, Hou and Wetton [7], Benjamim and Denny [24], Schreiber and Keller [25] and Shen [26], to mention only a few.

We assume $u = 0$ and $v = 0$ on all the fixed walls and that on the moving wall at $y = 1$, $u = 1$ and $v = 0$. These boundary conditions can be written

in terms of the stream function as

$$\psi = 0$$

on all boundaries and

$$\frac{\partial \psi}{\partial n} = \epsilon$$

where $\epsilon = 0$ on fixed walls and $\epsilon = 1$ on the moving wall at $y = 1$. The coordinate n is normal to the surface.

5.1. Stability. In the driven cavity problem, energy is provided to the system through forces acting on the moving wall and this energy is dissipated by viscous action, becoming heat which will be lost through the cavity walls. The driven cavity does not show stability for a Reynolds number larger than 7500, instead there is bounded oscillations of the energy even for very small time-steps. We have not analysed the nature of this oscillation, although the reasons may be associated with the dynamical features of the physical problem as reported in the literature for the driven cavity in papers such as Shen [26], Bruneau and Jouron [27] and Goodrich et al. [28], where other numerical schemes were used.

For the driven cavity problem, a steady laminar flow exists for $Re < 3000$. In this section we give calculations of the stability of numerical calculation of the steady state for a representative Reynolds number 350.

We consider the matrix formulation, described in section 2, of the system composed by the vorticity equation with the Poisson's equation. The velocity field $(\tilde{u}, \tilde{v})$ introduced in the vorticity equation is the numerical approximation velocity field to (u, v) that we obtain from numerical solution of the cavity flow problem.

When we use the second-order and third-order discretisation for the vorticity equation and for Thom, Alessio and Dennis and Briley vorticity boundary discretisations at Reynolds number 350, the result of the eigenvalues for the matrix formulation is described in figure 5. We have used the second-order Poisson's discretisation. Nevertheless if instead we use the fourth-order Poisson's discretisation the stability results are very similar to the ones presented in Figure 5.

5.2. Accuracy. There are well established calculations of the driven cavity problem which provide reference values for the solution. We use those from Bottela and Peyret [29] which were computed using a high order spectral

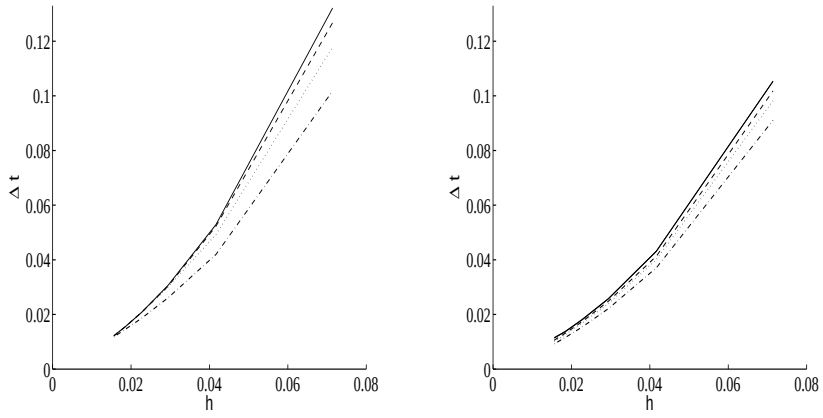

FIGURE 5. Unstable region for Re = 350 [above the curves]: eigenvalues larger than one; (a) For the 2nd order method (b) For the 3th order method. Thom's boundary condition (−); Alessio's boundary condition (−·−); Wood's and Briley's boundary condition (···); Jensen's boundary condition(−−).

method. In particular we examine the case $Re = 100$ and the value of the vorticity in the middle of the moving wall and the vorticity and stream-function in the center of the cavity. The results were considered converged for a variation of the vorticity between time steps of order 10^{-21}, that is the limit of double precision accuracy. We have used four meshes, 32×32, 64×64, 128×128 and 256×256. Then results from pairs of meshes were extrapolated to give an estimate of the convergence rate as the mesh size decreases. The results are given in tables 2-4. For most of the calculations the convergence rate is essentially quadratic. The exception is the condition from d'Allesion & Dennis where the convergence rate seems closer to 1.5. It is apparent that the choice of discretisation of the Poisson equation makes no difference, the conditions which gave quartic convergence in the previous section are now only quadratic so that the conditions for Bramble-Hubbard theory to allow global convergence to be determined by discretisation in the interior do not hold (recall that Quickest should be close to third order accurate in space so we might have hoped to find Quickest plus quartic discretisation of the Poisson equation giving close to third order convergence).

$\omega\|_{\partial\Omega}$	$\mathbf{u}\cdot\nabla\omega$	$\nabla^2\psi=-\omega$	$\omega(0.5,1)$ Reference=6.564094				Convergence		
			32×32	64×64	128×128	256×256	32-64	64-128	128-256
Thom	Lax Wendroff	$O(h^2)$	6.990319	6.659525	6.585685	6.569531	2.16	2.14	1.99
		$O(h^4)$	6.973841	6.650393	6.582504	6.568800	2.25	2.23	1.97
	Quickest	$O(h^2)$	6.856680	6.630311	6.581038	6.568237	2.14	1.97	2.03
		$O(h^4)$	6.838890	6.620976	6.577831	6.567307	2.27	2.05	2.10
Woods	Lax Wendroff	$O(h^2)$	6.856138	6.636151	6.581579	6.568751	2.02	2.04	1.91
		$O(h^4)$	6.833118	6.626328	6.578337	6.568015	2.11	2.13	1.86
	Quickest	$O(h^2)$	6.727854	6.607491	6.576985	6.567460	1.92	1.75	1.94
		$O(h^4)$	6.703616	6.597450	6.573714	6.566524	2.06	1.79	1.98
Jensen	Lax Wendroff	$O(h^2)$	6.851832	6.635290	6.581445	6.568735	2.01	2.04	1.90
		$O(h^4)$	6.831085	6.624681	6.577995	6.567962	2.14	2.12	1.85
	Quickest	$O(h^2)$	6.724270	6.606717	6.576860	6.567444	1.91	1.74	1.93
		$O(h^4)$	6.701177	6.595836	6.573376	6.566472	2.11	1.77	1.96
d'Allesio	Lax Wendroff	$O(h^2)$	6.915013	6.665129	6.592959	6.573593	1.80	1.81	1.60
		$O(h^4)$	6.889537	6.655285	6.589724	6.572859	1.84	1.83	1.55
	Quickest	$O(h^2)$	6.780886	6.635431	6.588223	6.572284	1.60	1.56	1.56
		$O(h^4)$	6.754719	6.625346	6.584954	6.571350	1.64	1.55	1.52
Briley	Lax Wendroff	$O(h^2)$	6.846822	6.638982	6.582381	6.568893	1.92	2.03	1.93
		$O(h^4)$	6.823843	6.627732	6.578811	6.567906	2.03	2.11	1.95
	Quickest	$O(h^2)$	6.721911	6.610509	6.577795	6.567601	1.77	1.76	1.97
		$O(h^4)$	6.696143	6.598940	6.574191	6.566612	1.92	1.79	2.00

Table 2. Calculation of wall vorticity midway along moving wall, $\omega(0.5,1)$, for four mesh resolutions together with extrapolated convergence rate for varying vorticity boundary condition, convection-diffusion and stream function-vorticity equation discretisation. The reference value given by Botella & Peyret (1998) is $\omega(0.5,1)=6.564094$. Numerical parameters are : $Re=100$, $\Delta t=0.0005$, multigrid residual less than 10^{-7}.

Boundary method	Convection Diffusion	Poisson Equation	$\omega(0.5,0.5)$ Reference=1.174412				Convergence		
			32×32	64×64	128×128	256×256	32-64	64-128	128-256
Thom	Lax-Wendroff	$O(h^2)$	1.063036	1.146349	1.166998	1.172601	1.99	1.92	2.03
		$O(h^4)$	1.087573	1.153773	1.169074	1.173216	2.07	1.95	2.16
	Quickest	$O(h^2)$	1.106146	1.157270	1.168431	1.173058	1.99	1.52	2.14
		$O(h^4)$	1.131313	1.164780	1.170514	1.173611	2.16	1.31	2.28
Woods	Lax-Wendroff	$O(h^2)$	1.081257	1.149183	1.167304	1.172618	1.88	1.83	1.99
		$O(h^4)$	1.106249	1.156676	1.169390	1.173229	1.94	1.82	2.09
	Quickest	$O(h^2)$	1.123390	1.160001	1.168729	1.173070	1.82	1.34	2.08
		$O(h^4)$	1.148942	1.167596	1.170825	1.173624	1.90	0.93	2.19
Jensen	Lax-Wendroff	$O(h^2)$	1.081077	1.149267	1.167335	1.172620	1.89	1.83	1.98
		$O(h^4)$	1.105883	1.156949	1.169465	1.173245	1.97	1.82	2.08
	Quickest	$O(h^2)$	1.122976	1.160052	1.168758	1.173078	1.84	1.34	2.08
		$O(h^4)$	1.148631	1.167852	1.170904	1.173040	1.97	0.90	1.35
d'Allesio	Lax-Wendroff	$O(h^2)$	1.063547	1.140899	1.163966	1.171173	1.73	1.68	1.69
		$O(h^4)$	1.088474	1.148362	1.166048	1.171759	1.72	1.64	1.66
	Quickest	$O(h^2)$	1.106677	1.151932	1.165426	1.171635	1.59	1.32	1.69
		$O(h^4)$	1.132078	1.159515	1.167520	1.172189	1.51	1.11	1.63
Briley	Lax-Wendroff	$O(h^2)$	1.081195	1.148418	1.167115	1.172590	1.84	1.83	2.00
		$O(h^4)$	1.106169	1.156240	1.169278	1.173146	1.91	1.82	2.02
	Quickest	$O(h^2)$	1.122568	1.159183	1.168539	1.173038	1.77	1.37	2.10
		$O(h^4)$	1.148513	1.167140	1.170713	1.173605	1.83	0.98	2.20

Table 3. Calculation of vorticity at the centre, $\omega(0.5,0.5)$, for four mesh resolutions together with extrapolated convergence rate for varying vorticity boundary condition, convection-diffusion and stream function-vorticity equation discretisation. The reference value given by Botella & Peyret (1998) is $\omega(0.5,0.5) = 1.174412$. Numerical parameters are : $Re = 100$, $\Delta t = 0.0005$, multigrid residual less than 10^{-7}.

Boundary method	Convection Diffusion	Poisson Equation	$\psi(0.5,0.5)$ Reference=0.0665474				Convergence		
			32×32	64×64	128×128	256×256	32-64	64-128	128-256
Thom	Lax-Wendroff	$O(h^2)$	0.062828	0.065634	0.066314	0.066490	2.03	1.97	2.02
		$O(h^4)$	0.063660	0.065884	0.066385	0.066510	2.12	2.03	2.13
	Quickest	$O(h^2)$	0.064146	0.065960	0.066355	0.066503	2.03	1.61	2.13
		$O(h^4)$	0.064976	0.066215	0.066426	0.066522	2.24	1.45	2.27
Woods	Lax-Wendroff	$O(h^2)$	0.063479	0.065729	0.066322	0.066490	1.91	1.86	1.96
		$O(h^4)$	0.064325	0.065982	0.066393	0.066510	1.97	1.88	2.04
	Quickest	$O(h^2)$	0.064746	0.066051	0.066363	0.066503	1.86	1.43	2.05
		$O(h^4)$	0.065596	0.066306	0.066434	0.066522	1.98	1.09	2.15
Jensen	Lax-Wendroff	$O(h^2)$	0.063483	0.065733	0.066324	0.066490	1.91	1.86	1.96
		$O(h^4)$	0.064322	0.065993	0.066396	0.066510	2.01	1.88	2.03
	Quickest	$O(h^2)$	0.064742	0.066054	0.066364	0.066503	1.87	1.43	2.05
		$O(h^4)$	0.065595	0.066317	0.066437	0.066523	2.05	1.06	2.15
d'Allesio	Lax-Wendroff	$O(h^2)$	0.062720	0.065385	0.066183	0.066429	1.72	1.68	1.63
		$O(h^4)$	0.063566	0.065636	0.066254	0.066450	1.71	1.63	1.58
	Quickest	$O(h^2)$	0.064039	0.065717	0.066226	0.066443	1.59	1.37	1.62
		$O(h^4)$	0.064885	0.065972	0.066297	0.066462	1.53	1.20	1.55
Briley	Lax-Wendroff	$O(h^2)$	0.063483	0.065701	0.066315	0.066488	1.86	1.87	1.98
		$O(h^4)$	0.064328	0.065966	0.066389	0.066508	1.93	1.88	2.00
	Quickest	$O(h^2)$	0.064722	0.066021	0.066356	0.066502	1.79	1.46	2.07
		$O(h^4)$	0.065587	0.066290	0.066430	0.066521	1.90	1.14	2.16

Table 4. Calculation of streamfunction at centre, $\psi(0.5,0.5)$, for four mesh resolutions together with extrapolated convergence rate for varying vorticity boundary condition, convection-diffusion and stream function-vorticity equation discretisation.
Numerical parameters are : $Re = 100$, $\Delta t = 0.0005$, multigrid residual less than 10^{-7}.

6. Conclusion

We have developed a global iteration matrix formulation for the stream-function vorticity equations and applied it to two driven cavity problems

to examine the effect on numerical stability of different numerical vorticity boundary conditions. The main conclusion is that the various ways of treating the boundary vorticity make little difference to stability which is determined mainly by the discretisation of the advection-diffusion vorticity equation. We have observed in passing some results for accuracy of the calculations and observe that there are situations where discretisation errors near the boundary do not propagate into the interior and do not affect the global accuracy, as given by Bramble–Hubbard theory but for the most part, in solution of practical problems using time marching schemes, it is difficult to exceed second order convergence.

References

[1] Ottino J. *The kinematics of mixing, stretching, chaos and transport*. Cambridge University Press, 1989.

[2] Thom A. The flow past a circular cylinders at low speeds. *Proc. Roy. Soc. London* 1933; **A141**:651–666.

[3] Roache P. *Computational Fluid Dynamics*. Hermosa, 1972.

[4] Peyret R. and Taylor T. *Computational methods for fluid flow*. Springer-Verlag: Berlin, 1986.

[5] Orszag S. and Israeli M. Numerical simulation of viscous incompressible flows. *Annual Review of Fluid Mechanics* 1974; **6**:281–318.

[6] Gresho P. Some interesting issues in incompressible fluid dynamics, both in the continuum and in numerical simulation. *Advances in applied mechanics* 1992; **28**:45–140.

[7] Hou T. and Wetton B. Convergence of a finite difference scheme for the Navier-Stokes equations using vorticity boundary conditions. *SIAM Journal of Numerical Analysis* 1992; **29**:615–639.

[8] Wang C. and Liu J. Analysis of finite difference schemes for unsteady Navier-Stokes equations in vorticity formulation. *Numer. Math.* 2002; **91**:543–576.

[9] Weinan E. and Liu J. Vorticity boundary condition and related issues for finite difference schemes. *Journal of Computational Physics* 1996; **124**:368–382.

[10] Napolitano M., Pascazio G., and Quartapelle L. A review of vorticity conditions in the numerical solution of the $\omega - \psi$ equations. *Computer and Fluids* 1999; **28**:139–185.

[11] Li Z. and Wang C. A fast finite difference method for solving Navier-Stokes equations on irregular domains. *Comm. Math. Sci* 2003; **1**:180–196.

[12] Spotz W. Accuracy and performance of numerical wall boundary conditions for steady, 2D incompressible stream function vorticity. *Int. J. Numerical Methods in Fluids* 1998; **28**:737–757.

[13] Sousa E. and Sobey I. Numerical stability of unsteady stream-function vorticity calculations. *Communications in Numerical Methods in Engineering* 2003; **19**:407–419.

[14] Richtmyer R. and Morton K. *Difference methods for initial-value problems*. Wiley-Interscience: New York, 1967.

[15] Sousa E. and Sobey I. A family of finite difference schemes for the convection-diffusion equation in two dimensions. In *enumath 2001 Numerical Mathematics and Advanced Applications*, pp 179–188. Springer-Verlag, 2002.

[16] Iserles A. *A first course in the Numerical Analysis of Differential Equations*. Cambridge University Press, 1996.

[17] Woods L. A note on the numerical solution of a fourth order differential equation. *Aeronautical Quarterly* 1954; **5**:176–182.

[18] Jensen V. Viscous flow round a sphere at low Reynolds numbers. *Proceedings of the Royal Society* 1959; **A294**:346–366.
[19] d'Alessio S. and Dennis S. A vorticity model for viscous flow past a cylinder. *Computers & Fluids* 1994; **23**:279–293.
[20] Briley W. A numerical study of laminar separation bubbles using Navier-Stokes equations. *Journal of Fluid Mechanics* 1971; **47**:713–736.
[21] Turkel E. Symmetric Hyperbolic difference schemes and Matrix Problems. *Linear Algebra and its Applications* 1977; **16**:109–129.
[22] Collatz L. *Numerische behandlung von differentialgleichungen*. Springer-Verlag, 1951.
[23] Bramble J. and Hubbard B. New monotone type approximations for elliptic problems. *Mathematics of Computation* 1964; **18**:349–367.
[24] Benjamin A. and Denny V. On the convergence of numerical solutions for 2-D flows in a cavity at large Re. *Journal of Computational Physics* 1979; **33**:340–358.
[25] Schreiber R. and Keller H. Driven cavity flows by efficient numerical techniques. *Journal of Computational Physics* 1983; **49**:310–333.
[26] Shen J. Hopf bifurcation of the unsteady regularized driven cavity flow. *Journal of Computational Physics* 1991; **95**:228–245.
[27] Bruneau C. and Jouron C. A new upwind scheme for the driven cavity flow. *C. R. des Academie des Sciences* 1988; **307**:359–362.
[28] Goodrich J., Gustafson K., and Halasi K. Hopf bifurcation in the driven cavity. *Journal of Computational Physics* 1990; **90**:219–261.
[29] Botella O. and Peyret R. Benchmark spectral results on the lid-driven cavity flow. *Computers & Fluids* 1998; **27**:421–433.

Ercília Sousa
Departamento de Matemática, Universidade de Coimbra, Portugal

Ian Sobey
Oxford University Computing Laboratory, U.K.